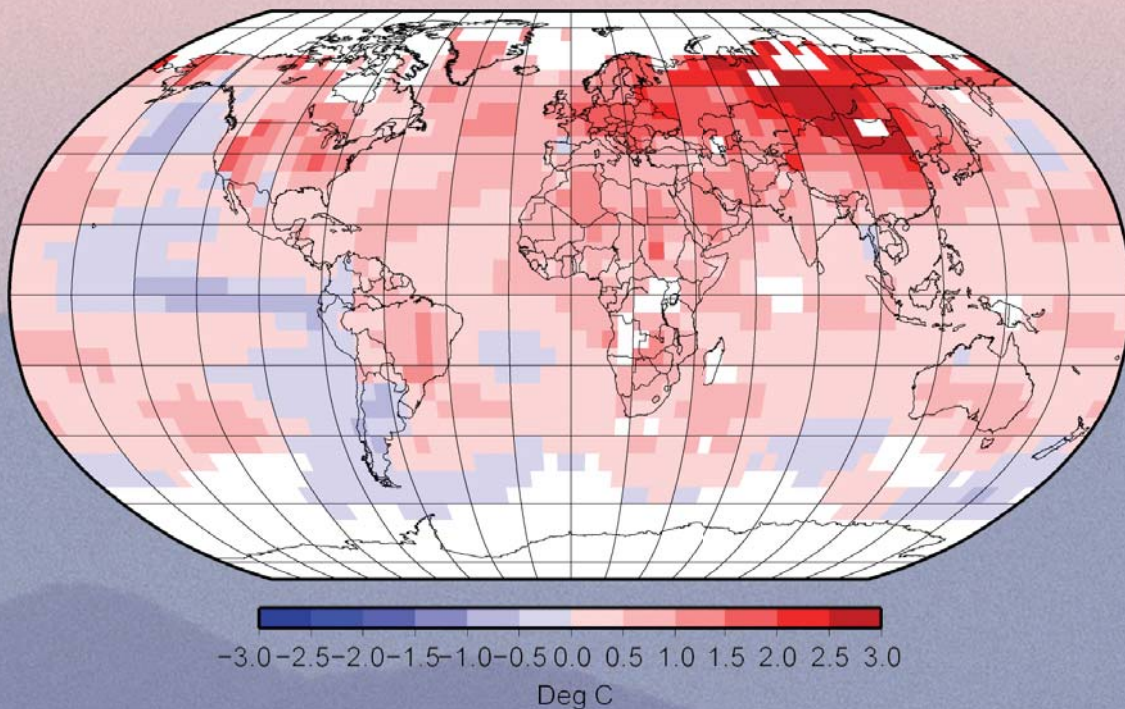


STATE OF THE CLIMATE IN 2007

D. H. LEVINSON AND J. H. LAWRIMORE, Eds.

ASSOCIATE Eds.: A. ARGUEZ, H. J. DIAMOND, F. FETTERER, A. HORVITZ, J. M. LEVY



Geographic distribution of global surface temperature anomalies in 2007, relative to the 1961 to 1990 average.

Special Supplement to the *Bulletin of the American Meteorological Society*
Vol. 89, No. 7, July 2008



of the water cycle under global warming. With the availability of continuous satellite-based ocean precipitation records from 1979, a link of evaporation with precipitation records would lead to a better understanding as to how global water cycle has changed in past decades.

4) TROPICAL CYCLONE HEAT POTENTIAL—G. J. Goni

The role of the ocean in TC formation has been largely recognized and accepted. The formation of Atlantic hurricanes has been linked to the SST, where values of this parameter larger than approximately 26°C have been shown to be a necessary but insufficient condition for hurricane cyclogenesis. Additionally, the intensification of hurricanes involves a combination of favorable atmospheric conditions, such as trough interactions and small vertical shear (DeMaria et al. 1993). After a series of events where the sudden intensification of hurricanes occurred when their path passed over oceanic warm features, it became clear that the upper ocean may play an important role in this process.

Although the sea surface temperature provides a measure of the surface ocean conditions, it gives no information about the subsurface (first tens of meters) ocean thermal structure. It is known that the oceanic skin temperature erodes when the sea surface is affected by strong winds, creating a well-mixed layer that can reach depths of several tens of meters. As the TC progresses, it travels above waters with mixed layer temperatures similar to their skin sea surface temperatures. This provides the motivation to investigate and monitor the upper-ocean thermal structure, which has become a key element in the study of tropical cyclone–ocean interactions focused

on prediction of sudden tropical cyclone intensification. Warm ocean features, mainly anticyclonic rings and eddies, are characterized by a deepening of the isotherms toward their centers with a markedly different temperature and salinity structure than the surrounding water mass. We present here results that are used to a) monitor the upper-ocean heat content in all basins where TCs occur, and b) investigate any possible link between this parameter and the growth of intense TCs during 2007.

The TCHP is the heat contained in the upper ocean from the sea surface to the depth of the 26°C isotherm. Hydrographic observations cannot provide TCHP fields needed to monitor this parameter on a daily to weekly basis with global coverage. Consequently, a methodology based on a combination of hydrographic and satellite-derived observations is used to create daily global fields of TCHP (Goni et al. 1996; Shay et al. 2000). Statistical analyses of these fields have shown that values of 50 kJ cm⁻² are usually needed for the ocean to have an effect on the intensification of an Atlantic hurricane (Mainelli et al. 2008). Clearly, areas with high values of TCHP may be important only when TCs travel over them.

There are seven basins where TCs occur: North Atlantic, east Pacific, west Pacific, north Indian, southeast Indian, southwest Indian, and South Pacific. Results presented separate the North Atlantic basin into tropical Atlantic and Gulf of Mexico. The TCHP anomalies are computed during the months of TC activity in each hemisphere: June through November in the Northern Hemisphere and November through April in the Southern Hemisphere. Anomalies are defined as departures from the mean TCHP obtained for the same months from 1993 to 2007. These anomalies show large variability within and among the basins (Fig. 3.9, left).

In the Pacific Ocean, the largest anomalies showed the signature of the negative phase of the 2007 ENSO event (La Niña). However, these anomalies are mostly outside regions where TCs occur, with the exception of the west Pacific and South Pacific basins. The west Pacific showed positive anomalies only, while the South Pacific showed both large positive and negative anomalies. The north Indian Basin exhibited positive values in the Arabian Sea and negative values in the Bay of Bengal. In the mean, the Gulf of Mexico and the tropical Atlantic exhibited small positive anomalies. Nevertheless, within the tropical Atlantic the anomalies were positive (negative) to the south (north) of approximately 25°N. The analysis of the monthly TCHP anomalies averaged over each basin since 1993 (Fig. 3.9) showed that the only two basins

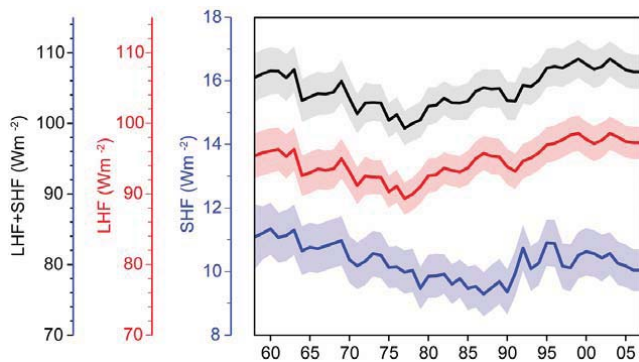


FIG. 3.8. Year-to-year variations of global averaged annual mean latent plus sensible heat flux (upper curve, black), latent heat flux (middle curve, red), and sensible heat flux (bottom curve, blue). The shaded areas indicate the upper and lower limits at the 90% confidence level.

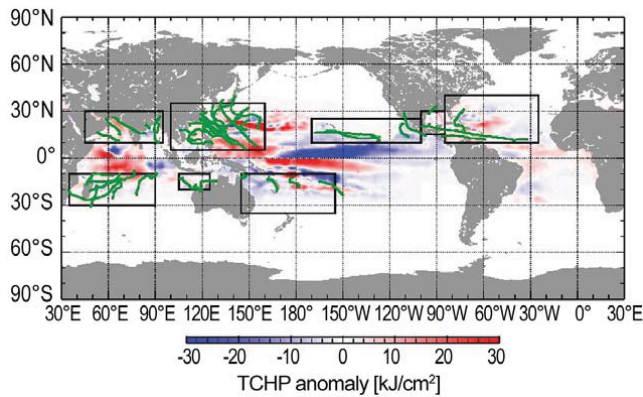
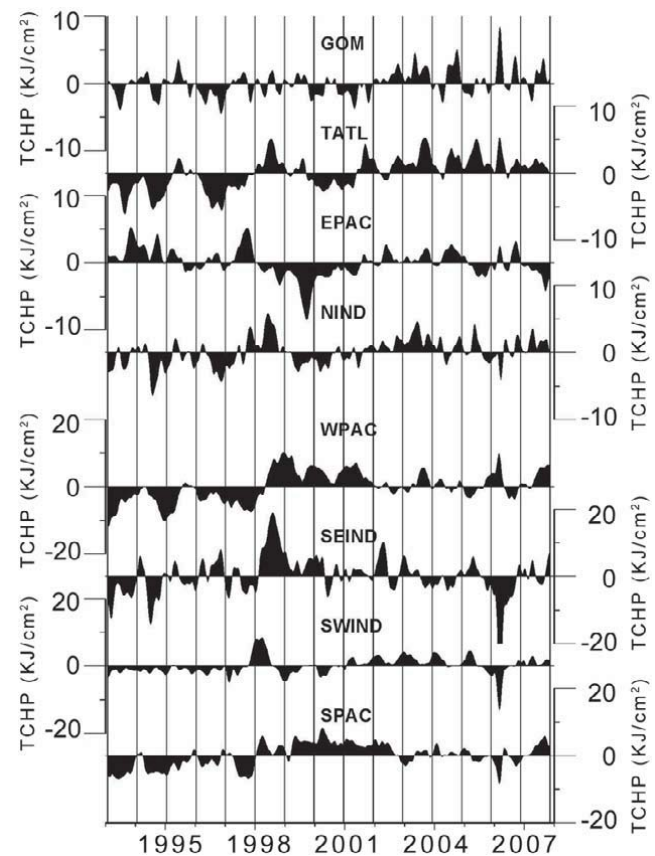


FIG. 3.9. (left) Global anomalies of TCHP corresponding to 2007 computed as described in the text. The boxes indicate the seven regions where TCs occur: from left to right, SWIND, NIND, WPAC, SEIND, SPAC, EPAC, and North Atlantic (shown as GOM and TATL separately). The green lines indicate the trajectories of all tropical cyclones category I and above from Nov 2006 to Apr 2007 in the Southern Hemisphere and Jun–Nov 2007 in the Northern Hemisphere. (right) Time series of monthly TCHP anomalies corresponding to each of the seven basins. Note that two different vertical scales are used in this figure.



exhibiting large monthly anomalies (within 75% of their historical extreme values) are the west Pacific and the South Pacific (Fig. 3.9, right). In the mean, all basins, except the eastern Pacific, showed mean positive annual values of TCHP during 2007.

Several TCs were identified to have gained strength when traveling into regions of very high values of TCHP. Some examples of these intensification events are shown in Fig. 3.10. The results presented here correspond to three intense (category 4 and 5) TCs, where the location of their intensification coincided with an increase of the values of TCHP along their tracks. Additionally, the cooling associated with the wake of the TCs is important since it influences the upper-ocean thermal structure on regional time scales within weeks to months after the passage of the cyclones. These TCs were Gonu in the north Indian Basin (Fig. 3.10, top three panels); Krosa in the west Pacific basin (Fig. 3.10, middle three panels); and Felix in the Caribbean Sea (Fig. 3.10, bottom three panels).

(i) Cyclone Gonu

During 3 June to 4 June 2007, cyclone Gonu, a storm with maximum winds of 104 mph (category 2), intensified to maximum sustained winds of 133 mph

(category 4). This cyclone intensified when traveling from a region with TCHP value of 60 kJ cm^{-2} over a mesoscale feature with TCHP values averaging 110 kJ cm^{-2} . The average decrease of TCHP and SST under the wake of this cyclone were of 25 kJ cm^{-2} and 3°C , respectively.

(ii) Typhoon Krosa

On 3 October 2007, Typhoon Krosa, a storm with maximum winds of 86 mph (category 1), intensified to one with maximum sustained winds of 138 mph (category 4). This typhoon traveled from a region with TCHP values of 30 kJ cm^{-2} over a mesoscale feature with TCHP values of 75 kJ cm^{-2} . The average decrease of TCHP and SST values under the wake of this typhoon were 50 kJ cm^{-2} and 3°C , respectively.

(iii) Hurricane Felix

On September 2, 2007, hurricane Felix, a cyclone with maximum winds of 104 mph (category 2), intensified to a hurricane with maximum sustained winds of 138 mph (category 4). This hurricane traveled from a region in the Caribbean Sea with TCHP values of 50 kJ cm^{-2} into a region with TCHP values of 110 kJ cm^{-2} . The average decrease of TCHP and SST values under the wake of this hurricane were

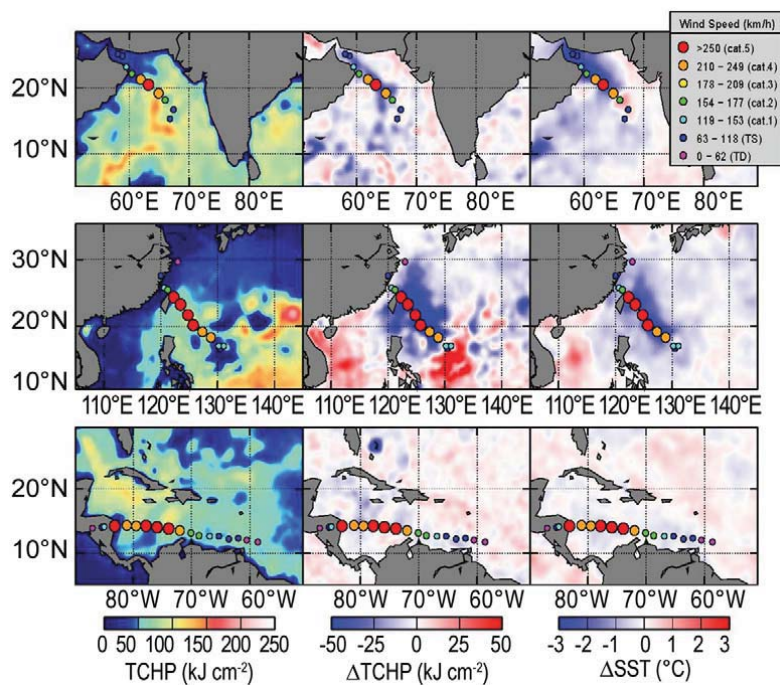


FIG. 3.10. (left) TCHP during three 2007 TCs: (top) Cyclone Gonu, (middle) Typhoon Krosa, and (bottom) Hurricane Felix; (center) TCHP cooling; and (right) SST cooling associated with the wake produced by each TC.

approximately 10 kJ cm^{-2} and 1°C , respectively. The cooling produced by this hurricane is substantially less than that produced by Cyclone Gonu and Typhoon Krosa, probably due to several factors such as translation speed of the storm and vertical ocean stratification.

Altimetry-derived fields of tropical cyclone heat potential provide a measure of the heat contained in warm mesoscale features. The examples presented here show the value of satellite-derived and in situ upper-ocean thermal observations for tropical cyclone intensity studies, suggesting that the inclusion of information on the upper-ocean thermal conditions in air–sea coupled models could help reduce the errors in intensity forecast.

c. Sea surface salinity—G. C. Johnson and J. M. Lyman

Ocean storage and transport of freshwater are intrinsic to many aspects of climate, including the global water cycle (e.g., Wijffels et al. 1992), El Niño (e.g., Maes et al. 2006), and global climate change (e.g., Held and Soden 2006). In the past, in situ ocean salinity data have been too sparse and their reporting too delayed for an annual global perspective of ocean freshwater, and its complement, salinity. However, over the past few years, the now mature Argo array of profiling floats, which measures temperature and salinity year-round in the upper 2 km of the ice-free

global ocean (Roemmich et al. 2004), has remedied this situation. The near-global Argo data are analyzed here to determine an annual average SSS anomaly for 2007 relative to a long-term climatology and to describe how annual SSS anomalies have changed in 2007 relative to 2006. Remote sensing of SSS by satellite is planned for 2010 (<http://aquarius.nasa.gov/>).

In this work the shallowest near-surface ($<25 \text{ m}$) salinity data flagged as good from each available Argo profile for 2006 and 2007 were subjected to a statistical check to discard outliers. After this statistical check, the remaining data were then cast as differences from a long-term climatological mean surface salinity field from the *World Ocean Atlas* based on historical data reported through 2001 (WOA2001; Boyer et al. 2002). The resulting anomalies were then mapped (Bretherton et al. 1976) assuming a Gaussian covariance function with 6° latitude and longitude decor-

relation length scales and a noise-to-signal variance ratio of 2.2. While some delayed-mode scientific controlled (final) Argo data are available for the 2006–07 time period, many real-time (preliminary) Argo data were used in both years. The real-time estimates of SSS made here could change after all the data have been subjected to careful scientific quality control.

SSS patterns are fairly well correlated with surface freshwater flux: the sum of evaporation, precipitation, and river runoff (e.g., Beránger et al. 1999) where advection processes are not dominant. In each ocean basin, subtropical salinity maxima centered between roughly 20° and 25° in latitude are signatures of the predominance of evaporation over precipitation. Conversely, in most regions where long-term climatological surface salinities are relatively fresh, precipitation generally dominates over evaporation. The 2007 anomalies from WOA2001 (Fig. 3.11) reveal some large-scale patterns. In 2007 the regions around the climatological salinity maxima are mostly salty with respect to WOA2001, as they were in 2006 (Arguez et al. 2007) and 2005 (not shown). In many of the climatologically fresh regions, 2007 values appear fresher than WOA2001, including: most of the ACC near 50°S , the subpolar gyre of the North Pacific, much of the ITCZ over the Atlantic and Pacific Oceans, and the South Pacific convergence zone west of about 165°W .